UNIUNEA EUROPEANĂ
GUVERNUL ROMÂNIEI
MINISTERUL MUNCII, FAMILIEI, PROTECȚIEI SOCIALE ȘI PERSOANELOR VÂRSTNICE
AMPOSDRU
Fondul Social European
POS DRU 2007-2013
Instrumente Structurale
2007-2013
MINISTERUL EDUCAȚIEI NAȚIONALE
OIPOSDRU
UNIVERSITATEA „ALEXANDRU IOAN CUZA“ din IAŞI

“Alexandru Ioan Cuza“ University
Faculty of Chemistry

Drd. Chim. **Adrian Iulian BORHAN**

Synthesis and characterization of spinel oxide compounds AB_2O_4

- DOCTORAL THESIS -

(Summary)

Scientific Coordinator
Prof. univ. dr. **Mircea Nicolae PALAMARU**

Iaşi, 2013

Keywords: oxides, ferrites, spinel, substitution, chromium, aluminum, lanthanum, IR spectroscopy, XRD, Mössbauer spectroscopy, VSM, dielectric permittivity, Orange I, photocatalytic degradation.

CONTENTS

Chapter I. General considerations on oxides with spinel structure

Chapter II. Synthesis and characterization of oxide compounds with spinel structure

II.3. The study of spinel oxide of the general formula $ZnFe_{2-x}Cr_xO_4 (0\leq x\leq 2)$

II.4. The study of spinel oxide of the general formula $ZnFe_{2-x}Al_xO_4(0\leq x\leq 2)$

II.5. The study of spinel oxide of the general formula $ZnFe_{2-2x}Cr_xAl_xO_4$

II.6. The study of spinel oxide of the general formula $ZnCr_{2-x}La_xO_4$ $(0\leq x\leq 2)$

Chapter III. The photocatalytic activity testing of the spinel oxides in the Orange I dye removal in aqueous solutions

INTRODUCTION

The possibility of using nanostructured materials for a wide range of superperfomant technological applications is of particular interest for scientific research and industrial production accordingly.

Oxides with spinel structure have played a decisive role in the magnetic materials group, but improvements and innovations continue to take place. In the last decade, numerous studies have been conducted in the field of nanocrystalline materials due to special properties and potential applications in magnetic and catalytic devices or microwave technology. Therefore, widely use in most modern technologies of these nanometric oxide compounds with magnetic, semiconductors, dielectrics and special catalytic properties justifies the choice of the research topic of the thesis.

Thee objective of the present research was to study the relationship between the method of preparation, the structural and magnetic, electrical and photo-catalytic properties of chromium-based spinel oxides. Therefore, we proposed to prepare new spinel oxides based on Cr, with nanoscale dimension and high purity at a temperature as low as possible using sol-gel auto-combustion method, for applications at high frequencies.

For this purpose, were prepared three series of oxide spinel with mixed valence, that having the general formula $ZnFe_{2-x}M_xO_4$, where M = Cr, Al and respectively, $ZnFe_{2-2x}Cr_xM_xO_4$ (M = Al). Finally, it was prepared rare earth substituted materials of the general formula $ZnCr_{2-x}M_xO_4$ (M = La). It is well known that the substitution of Cr^{3+} ions in the ferrites with spinel structure increases the electrical resistivity and decrease the dielectric loss, making the material ideal for high frequency applications. The Al^{3+}

substituted zinc ferrite may be used in a wide range of radio frequencies and microwave applications, in which is necessary that the electric and magnetic losses to be minimum. Lantaninde substitution is suitable for the reduction of Curie temperature and increasing the magnetic anisotropy and coercivity of materials [9]. However, as will be seen in the section dedicated to, the preparation of rare earth substituted materials is very difficult.

Experimentally stage in the laboratory MACS-Montpellier offered me the opportunity to test the applicability of the materials synthesized in photochemical decomposition of aqueous Orange I dye under UV light illumination. The literature contains few works about the photocatalytic properties of zinc ferrite substituted by trivalent cations in decomposition processes of dyes used in the industry.

The thesis is structured into two main parts, themselves composed of three chapters. For a better understanding of nanostructured materials with spinel structure, first part of the thesis includes generalities about the structure, preparation and physical properties of oxides with spinel structure and a summary of the most representative bibliographic information about the preparation and characterization of such oxides. The second part of the thesis consists of two main sections (II and III). Chapter II describes the synthesis protocol of nanomaterials based on chromium. Obtaining the desired materials was confirmed by the characterization techniques such as infrared spectroscopy, X-ray diffraction, electron microscopy, Mössbauer spectroscopy. Furthermore, it was investigated the effect of substitution with trivalent cations in the octahedral positions of ferrites on the magnetic and dielectric properties.

The chapter III presents the performance of the materials studied in fotodecomposition process of Orange I dye in aqueous solution under UV light irradiation. The materials that showed a high performance have been tested then in Orange I dye photodecomposition under visible light irradiation. Based on preliminary results was observed improving the photocatalytic activity by substitution with trivalent cations.

In the end of the thesis are presented the general conclusions of the research, references and valorisation of results.

Personal research were aimed the synthesis and characterization of spinel oxides based on chromium. Personal investigations covered proposed topics, and the results were presented as concisely as and clearly. Some of the results obtained in the research were published in specialized journals globally recognized and others are submitted for publication. The results obtained were valorized through presentations at various national and international conferences both in the poster session as well as the Plenary session.

Current state of knowledge

Chapter I. General considerations on oxides with spinel structure

I.1. The crystalline structure of spinel

Oxide compounds with spinel structure are part of a class of materials with high performance technological applications, which often does not exist sustainable alternative. The spinels forms one of major family of crystalline oxides. Their name comes from the mineral $MgAl_2O_4$, which has a homologous crystalline structure. The spinels with ideal structure crystallizes in cubic system (fcc), forming octahedral crystals belonging to space group Fd3m. Spinels group comprises about 30 minerals and main member of this family has general formula AB_2O_4. Tetrahedral position "A" can be occupied by divalent ions such as Mg, Fe, Ni, Mn and Zn. On the octahedral position "B" may be incorporated trivalent ions like Al, Fe, Cr and Mn. Oxygen ions are heavier than metal ions and therefore one can say that the spinel structure is a face-centered cubic lattice and showing two sublattices "A" and "B" [11]. Therefore, can be described three spinel structure arrangements:

a. *Normal spinel*, $[A]^{ted}[B_2]^{oct}O_4$

b. *Inverse spinel*, $[B]^{ted}[AB]^{oct}O_4$

c. *Mixed spinel*, $A_{1-\lambda}B_{\lambda}(A_{\lambda}B_{2-\lambda})O_4$

I.3. Synthesis methods of spinel oxides

The preparation of compounds in solid form is considered difficult and complex, although there are numerous synthesis methods: direct synthesis in solid phase (conventional ceramic process), co-precipitation method, hydrothermal method, combustion method, sol-gel method, etc.. The choice of method depends mainly on the form that we want the final compound. Main issue of of polycrystalline oxides preparation is the reproducibility properties required for industrial applications, because these properties are dependent on microstructure.

I.3.2.2. Combustion method

Combustion method proved to be one of the most advantageous methods of obtaining nanosized powders [24].It is a method recently applied in the synthesis of spinel oxides and therefore there are few studies on the preparation of chromium spinel oxides basis of this technique at low temperatures. Combustion techniques in solid phase present a series of advantages over the methods in solution, because of their simplicity and low degree of agglomeration. The method is based on a very exothermic redox reaction between the oxidizing metal salts such as metal nitrates and a combustion agent which is an organic compound (fuel), such as citric acid, tartaric acid, urea, polyacrylic acid, glycine, sucrose, etc. The use of such fuels has the advantage of obtaining fine powder which possesses the desired structural characteristics, by intimate mixing of the starting materials.

Personal contributions

Chapter II. Synthesis and characterization of oxide compounds with spinel structure

II.2.1. Synthesis of $ZnFe_{2-x}M_xO_4$ oxide compounds

The spinel oxide compounds synthesis with general formula $ZnFe_{2-x}M_xO_4$, where M= Cr and Al, were made by sol-gel auto-combustion method. The nanopowders with general formula $ZnFe_{2-x}Cr_xO_4$ (x = 0; 0,25; 0,5; 1,0; 1,5; 2,0) were prepared by using chromium nitrat [$Cr(NO_3)_3 \cdot 9H_2O$] (99,9%, Aldrich), iron nitrat [$Fe(NO_3)_3 \cdot 9H_2O$] (99,9%, Aldrich), zinc oxide ZnO (Sigma-Aldrich) and tartaric acid (Merck) as fuel agent. Zinc oxide was obtained in situ from ZnO (99%, Sigma-Aldrich) and nitric acid 20% solution.

$$ZnO + 2HNO_3 = Zn(NO_3)_2 + H_2O \qquad (1)$$

The tartaric acid was mixed with each sample of metal nitrates mixture in 3:1 molar ratio of tartaric acid to metallic cations, resulted from the following chemical equations proposed for the synthesis of $ZnFe_{2-x}M_xO_4$ ($0 \leq x \leq 2$) oxides:

$$Zn(NO_3)_2 + xM(NO_3)_3 + (2-x)Fe(NO_3)_3 + (11/2)O_2 + 3C_4H_6O_6 =$$
$$= ZnFe_{2-x}M_xO_4 + 8NO_2\uparrow + 12CO_2\uparrow + 9H_2O\uparrow \qquad (2)$$

In the case of our synthesis has been experimentally observed that auto-combustion ceases to occur at a molar ratio of nitrate: tartaric acid of 1:3 and therefore, this ratio can be taken as a fuel-deficient ratio. Thus we calculated as follows (Eq. 3):

Furthermore, we calculated fuel-deficient ratio (ρ) and obtained the value of 0.75, which proved adequate to obtain spinel oxides with high purity due to the presence of NO_3 groups, which provide a good oxidation and iron in high oxidation state, i.e. Fe^3

After coresponding salts solubilisation and tartaric acid adition, the solutions were heated at 70^0C through gel phase transformation. The gel was gradually heated at 350^0C, when the autocombustion occured. The obtained powders were presintered at 500^0C/7 h and then were sintered at 700^0C/7 h. The mixed solutions were heated for 3 h at 80^oC through gel phase transformation. The gel was heated at 300^oC, when the auto-ignition was clearly observed. The obtained powders **thermally treated in powder** in two steps: up to 500^0C/7 h and up to 700^0C/14 h.

II.3. The study of spinel oxides with general formula $ZnFe_{2-x}Cr_xO_4 (0 \leq x \leq 2)$

II.3.1. Overview

According to our literature searches, there is no report about $ZnFe_{2-x}Cr_xO_4$ synthesis by sol-gel auto-combustion. Our main objective was to synthesize pure nanocrystalline powders with the general formula $ZnFe_{2-x}Cr_xO_4$ (x=0, 0.25, 0.5, 1.0, 1.50, 2.0) by sol-gel auto-combustion method using tartaric acid as chelating and fuel agent and to investigate the effect of Cr^{3+} substitution in $ZnFe_2O_4$ on structural characteristics, magnetic and electrical properties.

II.3.2. Structural analysis by IR

The figure 14 presents IR spectra of $ZnFe_{2-x}Cr_xO_4$ $(0 \leq x \leq 2)$ nanomaterials in the wavenumber range 700 - 300 cm^{-1} to highlight lattice vibration modes. The presence of two main absorbtion peaks $\bar{\upsilon}_1$ and $\bar{\upsilon}_2$, characteristic of spinel structure is confirmed for all samples. These two peaks could suggest the existence of the spinel-type structure. Absobtion peak observed in the range 610-520 cm^{-1} is assigned to $\bar{\upsilon}_1$ wavenumber and that of range 490-390 cm^{-1} is attributed to $\bar{\upsilon}_2$ wavenumber [82]. Prezenţa celor două maxime de absorbţie corespunzătoare numerelor de undă $\bar{\upsilon}_1$ şi $\bar{\upsilon}_2$, caracteristice structurii de tip spinel este confirmată pentru toate probele preparate. Maximul de absorbţie din intervalul 520-610 cm^{-1} este atribuit numărului de undă $\bar{\upsilon}_1$ iar cel din domeniul 390-490 cm^{-1} este atribuit numărului de undă $\bar{\upsilon}_2$ [82]. The spectrum shows a shift of position peaks in both $\bar{\upsilon}_1$ and $\bar{\upsilon}_2$ wavenumbers with incresing of Cr content in system.

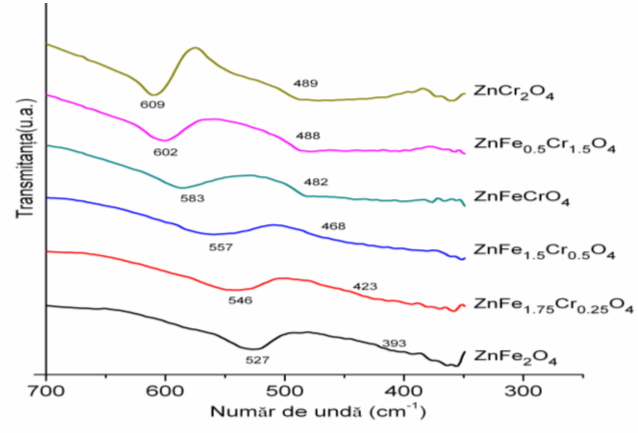

Figure 14. IR spectra of $ZnFe_{2-x}Cr_xO_4$ powders heated at 700°C

Table 1 shows the increase of force constant corresponding to tetrahedral and octahedral positions with increasing the amount of chromium in the system, which means a shortening of cation-oxygen bonds in both tetrahedral and octahedral units.

Table 1. IR wavenumbers ($\bar{\upsilon}_1$ and $\bar{\upsilon}_2$), force constants (K_T and K_O) and ($\bar{\upsilon}_1$-$\bar{\upsilon}_2$) difference

Composition (*x*)	$\bar{\upsilon}_1$ (cm^{-1})	$\bar{\upsilon}_2$ (cm^{-1})	K_T x10^5 (dynes/cm^2)	K_O x 10^5 (dynes/cm^2)	$\bar{\upsilon}_1$-$\bar{\upsilon}_2$
0,00	527	393	1,35	0,92	134
0,25	546	423	1,36	1,08	123
0,50	527	468	1,47	1,28	89
1,00	583	482	1,59	1,34	101
1,50	602	488	1,69	1,71	114
2,00	609	489	1,82	1,32	120

II.3.3. Structural analysis by X-ray diffraction

Figure 16 depicts the XRD patterns of $ZnFe_{2-x}Cr_xO_4$ compounds thermally treated up to 700^{0}C for 14 h, clearly seen the stabilization of spinel structure. Spinel monophase completion was observed for all samples, only for $ZnFe_{1.75}Cr_{0.25}O_4$ sample have been detected two secondary phases ZnO with hexagonal structure (89-0510, ICDD) and Fe_2O_3 with rhombohedral structure (89-0599, ICDD). These impurities occurs because of lower content of fuel agent.

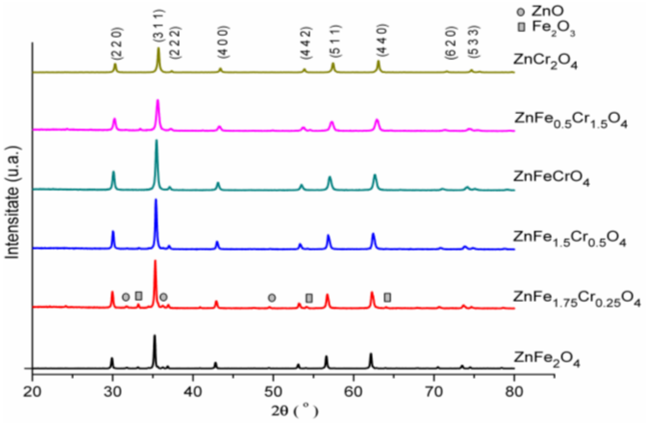

Figure16. X-ray diffraction patterns for $ZnFe_{2-x}Cr_xO_4$ powders heated at 700°C.

Table 2 shows a linear decrease of the lattice constant values and respectively, of the crystallite size in the range of 36-24 nm as a result of chromium content increase in the system. This variation in unit cell size can be due to the replacement of Fe^{3+} (0.645Å) ions by Cr^{3+} ions, a slightly smaller ion (0.615Å) [74].

Table 2. Structural parameters of $ZnFe_{2-x}Cr_xO_4$ powders ($0{,}0 \le x \le 2{,}0$)

Composition (x)	a_{311} (Å) ± 0.2%	D (nm) ± 0.5%	d_{311} (Å) ± 0.2%	X-ray density (dx) g/cm^3
0,00	8,404	35,5	2,53	5,42
0,25	8,397	33,8	2,53	5,39
0,50	8,377	32,5	2,52	5,40
1,00	8,347	28,2	2,51	5,41
1,50	8,311	24,5	2,50	5,44
2,00	8,291	27,4	2,50	5,44

For the $ZnFe_{2-x}Cr_xO_4$ system, known preference of Cr^{3+} ions for the octahedral sites [89,90], could be proposed the next cation distribution formula:

$$(Zn_y^{2+}Fe_{1-y}^{3+})^A[Zn_{1-y}^{2+}Fe_{1-x+y}^{3+}Cr_x^{3+}]^BO_4^{2-}$$

indicating that the Fe ions have migrated from the B to A sites (Table 3).

Table 3. Cation distribution, theoretical lattice parameter (a_{th}), bond lenght (R_A and R_B) and oxygen positional parameter (u)

x	a_{th}(Å)	R_A (Å)	R_B (Å)	Cation distribution	u^{43m} (Å)	$u^{\bar{3}m}$(Å)
0,00	8,442	1,9635	2,0321	$(Zn_{0,85}^{2+}Fe_{0,15}^{3+})$ $[Zn_{0,15}^{2+}Fe_{1,85}^{3+}]$	0,384	0,2594
0,25	8,429	1,9580	2,0307	$(Zn_{0,80}^{2+}Fe_{0,20}^{+})$ $[Zn_{0,20}^{2+}Fe_{1,55}^{3+}Cr_{0,25}^{3+}]$	0,384	0,2592
0,50	8,417	1,9525	2,0293	$(Zn_{0,75}^{2+}Fe_{0,25}^{3+})$ $[Zn_{0,25}^{2+}Fe_{1,25}^{3+}Cr_{0,50}^{3+}]$	0,384	0,2590
1,00	8,395	1,9470	2,0242	$(Zn_{0,70}^{2+}Fe_{0,30}^{3+})$ $[Zn_{0,30}^{2+}Fe_{0,70}^{3+}Cr_1^{3+}]$	0,384	0,2590
1,50	8,373	1,9415	2,0191	$(Zn_{0,65}^{2+}Fe_{0,35}^{3+})$ $[Zn_{0,35}^{2+}Fe_{0,15}^{3+}Cr_{1,50}^{3+}]$	0,384	0,2589
2,00	8,368	1,9800	1,9950	$(Zn_1^{2+})[Cr_1^{3+}Cr_1^{3+}]$	0,386	0,2618

II.3.4. Structural analysis by scanning electron microscopy

SEM microstructure for samples with composition x = 0.0, 0.5, 1.0, 2.0 are shown in **figure 17(a-d).** It can be seen that the grains of uniform size are distributed throughout the surface and shows the decreasing trend with chromium substitution. The particle size decrease significantly with increasing chromium concentration since the ionic radius of chromium is smaller than the ionic radius of iron. Also, the particles agglomerate with increasing chromium content. The average particle size is between 56-73 nm, which is slightly larger than that determinate by XRD. This shows that every particle is formed by a number of crystallites or grains [92].

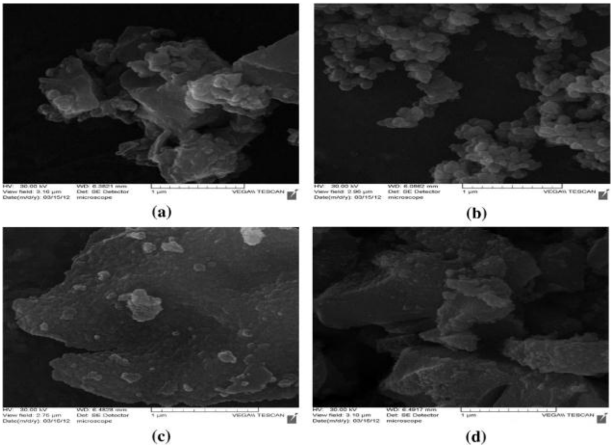

Figura 17(a-d). SEM micrographs of $ZnFe_{2-x}Cr_xO_4$: (a) x=0.0, (b) x=0.5, (c) x=1.0, (d) x=2.0

II.3.5. Magnetic properties study

Figure 19 shows typical hysteresis loop of investigated samples $ZnFe_{2-x}Cr_xO_4$ calcined at 700°C.

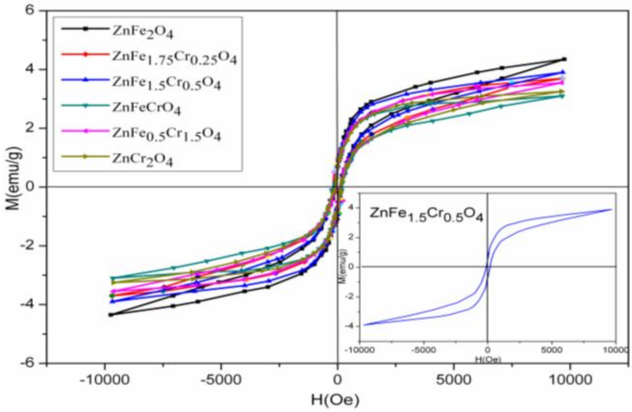

Figure 19. Hysteresis loop of $ZnFe_{2-x}Cr_xO_4$ serie

It can be seen that all investigated compounds produce a very narrow hysteresis cycle, indicating a behavior characteristic of soft magnetic materials. The saturation magnetization and coercitive field decrease nonlinearly with increase in chromium content because of cation distribution, microstructure, density powder and surface spin disorder. (Tabel 6).

Table 6. Magnetic parameters measured at room temperature and calculated for $ZnFe_{2-x}Cr_xO_4$ powders

Composition (x)	M_s (emu/g)	M_r (emu/g)	M_r/M_s	H_c (Oe)	μ_{exp} (magneton Bohr)	μ_{calc} (magneton Bohr)	Canting angle (°)
0,00	4,35	0,7	0,50	50	1,87	9,25	-
0,25	3,70	0,7	0,26	150	1,59	8,75	31,30
0,50	3,90	0,7	0,48	150	1,67	6,00	50,09
1,00	3,10	0,7	0,32	130	1,31	5,00	79,21
1,50	3,55	0,7	0,25	90	1,49	3,50	97,74
2,00	3,25	0,7	0,24	110	1,35	6,00	121,43

The low values of remanent magnetization M_r can be due to the nanosize crystallites and low saturation magnetization. The calculated values of M_r/M_s loop squareness ratio are less than 0.50, recommended materials to be used for cores and coils with low inductance [98].

II.3.6. Dielectric properties study

The real part of dielectric constants (ε') and imaginary part (ε") decreases with increasing frequency due to Maxwell-Wagner type interfacial polarization in accordance with Koop's phenomenological theory [60, 61] (figure 20 (a-b)). Chromium ions do not participate in the conduction process but decrease the number of electron hopping ($Fe^{3+} \leftrightarrow Fe^{2+}$) through which the electrons move in the direction of the electric field applied [99]. Dispersion of dielectric constant is maximum for composition x=0.5, $ZnFe_{1,5}Cr_{0,5}O_4$.

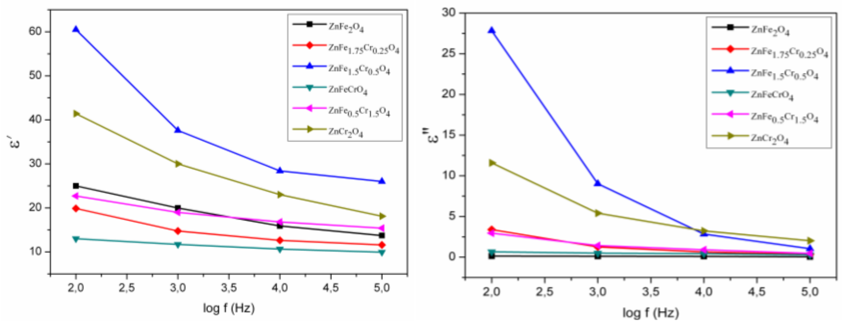

Figure 20(a-b). Variation of real (a) and complex (b) dielectric constant with frequency

Figure 21 shows that all tested compounds have a normal dielectric behavior and an exponential decrease in dielectric loss tangent values with increasing frequency, resulting in very low loss factors ranging from 0.02 to 0.04 at high frequencies.

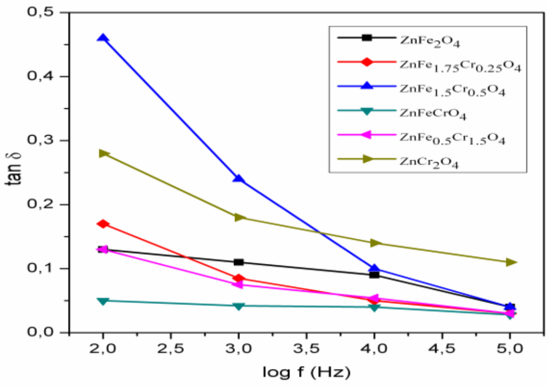

Figure 21. Variation of loss tangent, tanδ, with frequency

II.3.7. Conclusions

In this chapter we successfully studied the influence of introduction of Cr^{3+} ions in octahedral position B on the structure and magnetic and electrical properties of zinc ferrite.

It was optimized synthesis of chromium substituted zinc ferrite by the sol-gel auto-combustion, using a deficiency of fuel agent which contributed to the lower cost of synthesis.

Dielectric properties of the starting material were improved by the substitution of chromium ions. The dielectric constant and dielectric loss decrease with increase in frequency and attains a constant value at high frequencies.

These results indicate that Cr-substituted zinc ferrites are advised to be used in applications that require lower magnetic losses.

Capitolul III. Testarea activităţii fotocatalitice a oxizilor cu structură de tip spinel

III.2. Photocatalytic reaction procedure

The photocatalytic activity of the catalysts prepared was evaluated by degradation of recalcitrant textile dye Orange I (Tropaeolin 000 No.1) with chemical formula $C_{16}H_{11}N_2NaO_4S$ (d = 13.9Å) under UV-light irradiation. The photocatalytic degradation experiments were performed into a Pyrex cylindrical photo-reactor. A low pressure Hg lamp (Philips, Netherlands) emitting a wavelength of 185 nm was positioned at the centre of the reactor and was used for photoreaction under UV light. In each experiment, the reaction suspension was prepared by adding 0.40 g of catalyst powder into 75mL Orange I solution with a initial concentration of 80 mg/L and pH=3. The suspension was magnetically stirred in the dark for 30 min to reach adsorption-desorption equilibrium at constant temperature prior to irradiation, and then the solution was irradiated at differrent time. For comparison purposes, the photoreaction under visible light irradiation was performed using a 400W high pressure sodium lamp (APF, IP65, Italy) with main emission in the range of 400-800 nm, for the $ZnFe_{0.50}Cr_{1.50}O_4$ sample only, using the same protocol described before.

III.3.3. Use of the catalyst $ZnFe_{0,50}Cr_{1,50}O_4$ in removal process of the Orange I dye

Figure 51(a-b) shows the changes of the optical densities of 475 nm (–N = N–), 330 nm, 290 nm (naphthalene ring) and 240 nm (benzene ring) bands of orange I at different illumination time under UV light and visible light in the presence of $ZnFe_{0.50}Cr_{1.50}O_4$ powder. The photodegradation rate of Orange I over $ZnFe_{0.50}Cr_{1.50}O_4$ nanoparticles increases rapidly with increasing UV irradiation time, and reaches 92,80% in 45 min. Nevertheless, the decolorization rate under visible light is two times lower, ie 49% in 45 min.

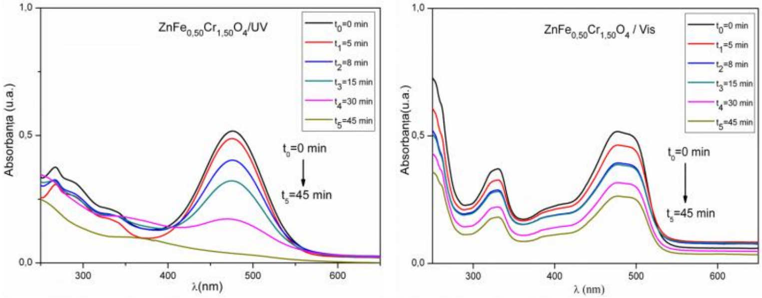

Figure 51(a-b). The change of absorbtion spectra of Orange I in presence of $ZnFe_{0.50}Cr_{1.50}O_4$ under UV/visible irradiation

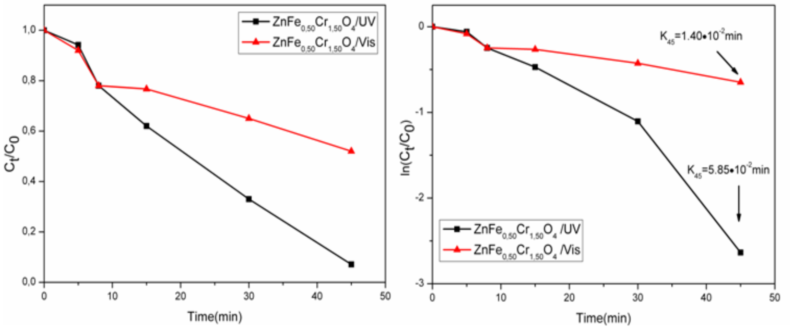

Figure 52(a- b). The degradation rate of Orange I over $ZnFe_{0.50}Cr_{1.50}O_4$ under UV/visible irradiation

The degradation kinetics of Orange I on $ZnFe_{0.50}Cr_{1.50}O_4$ catalyst under UV light and visible light could be analyzed by the first order kinetic model (figure 52(a-b)).

The best photocatalytic performance was achieved after 45 min of UV light iradiation, with first order kinetic rate constant k of $5.85 \cdot 10^{-2}$ min^{-1}. Under visible light, the first order kinetic rate constants k was about 4 times lower, ie $k = 1.54 \cdot 10^{-2}$ min^{-1}. $ZnFe_{0.50}Cr_{1.50}O_4$ catalyst shows a performance twice higher than TiO_2, but comparable with those of RE^{3+} (Sm^{3+}, Nd^{3+}, Pr^{3+}) doping in TiO_2 for Orange I dye degradation under UV light [135].

III.3.4. Conclusions

The photocatalytic process was promoted when Fe^{3+} cations were subtituted with Cr^{3+} cations. Therefore, the dye removal efficiency was enhanced up to 92.8% for x = 1.50 showing that $ZnFe_{0.50}Cr_{1.50}O_4$ material contains chromium optimal dosage for photocatalytic degradation of Orange I. The decolorization rate under visible light is two times lower that afforted under UV light.

General conclusions

- The study of both soft magnetic materials and dielectric materials is important because of the large number of applications in which they find useful. As I presented in the introduction, the literature contains numerous studies on these materials, aiming to obtain new materials with some practical features.
- In Part I of this thesis have been approached theoretical aspects regarding oxide materials with spinel structure. Have been described ideal spinel structure, possible types of structures and the relationship between the structure and the magnetic/electrical properties by incorporating a trivalent cation in octahedral sublattice of zinc ferrite.

- In this study, the sol-gel auto-combustion was used for the first time for the preparation of Cr, Al, and Cr-Al substituted zinc ferrite and La substituted zinc chromite. It has proved economic and effective.
- We managed to reduce the costs of high purity spinel oxide preparation by using a deficiency of combustion agent.
- The purity of phases obtained was confirmed by IR spectroscopy, X-ray diffraction, Mössbauer spectroscopy and scanning electron microscopy.
- XRD analysis confirmed the formation of spinel structure for all powders prepared showing a lattice constant decreasing trend with increasing substitution, which is due to the majority occupancy of octahedral positions in the spinel lattice. This variation is consistent with the proposed cation distribution in accordance with X-ray diffraction data. It was determined that B-B interactions increase while A-B and A-A interactions decrease with co-substitution and substitution of Cr^{3+} and Al^{3+} ions in the system.
- The incorporation of lanthanum cations in zinc chromite lattice by complete substitution of Cr^{3+} with La^{3+} has proven extremely difficult. Therefore, the substitution of large amounts of lanthanum ($x = 0.25$, 0.50, 1.00, 1.50 and 2.00) did not lead to the formation of spinel-type ferrite, but particularly surprising, were obtained double perovskite oxides for compositions in lanthanum $x = 0.25$ and 0.50, and mixtures of phases such as oxides of lanthanum ($ZnLaO_2$ and La_2O_3) for $x = 1.0$ and perovskite-type phases for compositions with $x = 1.50$ and 2.0.
- SEM micrographs showed that the particle size decreases with increasing substitution degree in all the series of spinels prepared, due to the decrease in B-B octahedral bond, resulting in particles less than 100 nm.

- Mössbauer spectra, recorded for zinc ferrite substituted with aluminum and co-substituted with Cr-Al, exhibit a central doublet which has been attributed to Fe^{3+} located in the octahedral sites of structure, which do not participate in the long-range magnetic ordering due to a large number of nonmagnetic nearest neighbors. During the preparation, it was obtained an unstable hematite phase on surface, or the segregation of α-Fe_2O_3 suggests the existence of a nanocrystalline phase, ZnO (undetected in XRD), that will react with hematite to form zinc ferrite at increasing temperature.
- In case of Cr-Al co-substituted zinc ferrite, the sample with $x = 0.50$, indicates a segregation of hematite by 72%. The remaining samples indicate complete transformation of hematite, α-Fe_2O_3, in the paramagnetic state of iron, i.e. $ZnFe_2O_4$ or $ZnFe_{2-2x}Cr_xAl_xO_4$, indicating that pure compounds were obtained.
- The relationship between the synthesis, the structure features and the magnetic and electric properties have been established.
- Therefore, the magnetization and coercitive field were found to decrease linearly with increasing Cr, Al and Cr-Al content, which has been explained by effective magnetic interaction (A-O-A, A-O-B and B-O-B). The lowest values of remanent magnetization M_r indicate that these materials can be used to manufacture cores and coils with low inductance.
- It is clear, also, the influence of the introduction of diamagnetic lanthanum ions on the magnetic properties of zinc chromite. It has been observed decrease in magnetization with increasing the content of lanthanum in the lattice both the at 300 K as well as 2K. A very interesting observation is that the saturation magnetization increases with decreasing temperature from 300K to 2K.

- Introduction of trivalent cations in zinc ferrite caused a number of changes in the spinel lattice, which have helped improve the dielectric properties. All the materials tested showed a normal dielectric behavior, in the sense that the permittivity and dielectric losses of zinc ferrite substituted with trivalent cation decreased by increasing the frequency of the AC field applied. This behavior can be explained by the conduction mechanism, which is due to electron transfer $Fe^{3+} \leftrightarrow Fe^{2+}$ between cations of different valence from the positions B. For high frequencies the dielectric loss values are very low, ranging between 0.02-0.04 for $ZnFe_{2-x}Cr_xO_4$ and $ZnFe_{2-x}Al_xO_4$ systems and respectively, 0.03 to 0.08 for $ZnFe_{2-2x}Cr_xAl_xO_4$ system. These features are very important for the possible manufacture of electronic devices that could be operated successfully in broad frequency range.
- The introduction of Cr^{3+} and Al^{3+} cations in the $ZnFe_2O_4$ spinel matrix, in the studied proportions, was able to promote the photodecomposition process of Orange I dye.
- The photocatalytic activity of pure spinel phase $ZnFe_{2-x}Cr_xO_4$ powders indicate the best dye removal efficiency for x = 1.50 sample, i.e. ≈92,80%. The decolorization rate under visible light is two times lower that afforted under UV light. Hence, nanoparticles of $ZnFe_{0.50}Cr_{1.50}O_4$ can act as photocatalyst of the degradation of azo dyes in an aqueous solution.
- The photocatalytic activity of pure spinel phase $ZnFe_{2-x}Al_xO_4$ was successfully employed, for the first time, on Orange I degradation under UV/visible light. The best photocatalytic performance, ie 65,53 %, was obtained for x=1,0 sample. $ZnFeAlO_4$ achieved the best photocatalytic performance after 45 min of UV light iradiation, with k of $2{,}37 \cdot 10^{-2}$ min^{-1},

which was 2.73 times as great as that over $ZnFe_2O_4$ nanoparticles ($k = 1.0 \cdot 10^{-2}$ min^{-1}).

- $ZnFe_{1,75}Cr_{0,125}Al_{0,125}O_4$ catalyst showed the best photocatalytic performance after 45 min of UV light iradiation, with k of $2,3 \cdot 10^{-2}$ min^{-1}, which was 2.3 times as great as that over $ZnFe_2O_4$ nanoparticles ($k = 1.0 \cdot 10^{-2}$ min^{-1}).
- I believe that the results presented in this thesis represents the starting point in solving other problems that may occur in practice. Soft magnetic materials produced can replace the ferrite cores used in the production of inductive components. The inductive components can be designed lighter, smaller, cheaper and more durable, leading to increasing performance of devices which can operate at very high frequencies.

Selected Bibliography

[12] R. Valenzuela, Novel applications of ferrites, Physics Research International, 2012 (2012).
[13] K.E. Sickafus, J.M. Wills, N.W. Grimes, Structure of spinel, Journal of the American Ceramic Society, 82 (1992) 3279-3292.
[14] A.R. West, *Basic Solid state Chemistry*, J.W.& D. Ltd 1999.
[15] H.P.J. Wijn, J. Smit, *Ferrites-Physical Properties of Ferrimagnetic Oxides in Relation to their Technical Applications*, John Wiley and Sons, Netherland, 1959, pp. 136-145.
[16] V. Lakhani, T. Pathak, N. Vasoya, K. Modi, Structural parameters and X-ray Debye temperature determination study on copper-ferrite-aluminates, Solid State Sciences, 13 (2011) 539-547.
[17] L. Zhang, Preparation of multi-component ceramic nanoparticles, Ohio State University, (2004).
[24] S.T. Aruna, A.S. Mukasyan, Combustion synthesis and nanomaterials, Current opinion in solid state and materials science, 12 (2008) 44-50.

[27] P. Hankare, R. Patil, K. Garadkar, R. Sasikala, B. Chougule, Synthesis, dielectric behavior and impedance measurement studies of Cr-substituted Zn–Mn ferrites, Materials Research Bulletin, 46 (2011) 447-452.

[29] M. Gabal, Y. Al Angari, Low-temperature synthesis of nanocrystalline NiCuZn ferrite and the effect of Cr substitution on its electrical properties, Journal of Magnetism and Magnetic Materials, 322 (2010) 3159-3165.

[30] A. Costa, V. Silva, H. Ferreira, A. Costa, D. Cornejo, R. Kiminami, L. Gama, Structural and magnetic properties of chromium-doped ferrite nanopowders, Journal of Alloys and Compounds, 483 (2009) 655-657.

[33] J. Toledo, M. Valenzuela, P. Bosch, H. Armendariz, A. Montoya, N. Nava, A. Vazquez, Effect of AI^{3+} introduction into hydrothermally prepared $ZnFe_2O_4$, Applied Catalysis A: General, 198 (2000) 235-245.

[34] S. Patange, S.E. Shirsath, B. Toksha, S.S. Jadhav, K. Jadhav, Electrical and magnetic properties of Cr^{3+} substituted nanocrystalline nickel ferrite, Journal of Applied Physics, 106 (2009) 023914-023917.

[35] R.K. Sharma, O. Suwalka, N. Lakshmi, K. Venugopalan, A. Banerjee, P. Joy, Synthesis of chromium substituted nano particles of cobalt zinc ferrites by coprecipitation, Materials Letters, 59 (2005) 3402-3405.

[36] C. N. R. Rao, B. Raveau, *Transition Metal Oxides. Structure, Properties and Synthesis of Ceramic Oxides*, Second Edition, John Wiley & Sons, New York, 1998.p. 4-29, 38-90, 240-251, 257-261, 292-300, 300-313, 323-360.

[37] R. Waldron, Infrared spectra of ferrites, Physical Review, 99 (1955) 1727.

[38] P. Hankare, R. Patil, U. Sankpal, S. Jadhav, K. Garadkar, S. Achary, Synthesis and morphological study of chromium substituted Zn–Mn ferrites nanostructures via sol–gel method, Journal of Alloys and Compounds, 509 (2011) 276-280.

[46] E. Casbeer, V.K. Sharma, X.-Z. Li, Synthesis and photocatalytic activity of ferrites under visible light: a review, Separation and Purification Technology, 87 (2012) 1-14.

[52] A.R. West, Solid state chemistry and its applications, (1984) pp.553-582.

[60] R. Hilborn, Maxwell-Wagner Polarization in Sintered Compacts of Ferric Oxide, Journal of Applied Physics, 36 (1965) 1553-1557.

[61] C. Koops, On the dispersion of resistivity and dielectric constant of some semiconductors at audiofrequencies, Physical Review, 83 (1951) 121.
[62] M. Gabal, Y.A. Angari, Effect of chromium ion substitution on the electromagnetic properties of nickel ferrite, Materials Chemistry and Physics, 118 (2009) 153-160.
[63] A. Birajdar, S.E. Shirsath, R. Kadam, S. Patange, K. Lohar, D. Mane, A. Shitre, Role of Cr^{3+} ions on the microstructure development, and magnetic phase evolution of $Ni_{0.7}Zn_{0.3}Fe_2 O_4$ ferrite nanoparticles, Journal of Alloys and Compounds, 512 (2012) 316-322.
[89] R.K. Sharma, V. Sebastian, N. Lakshmi, K. Venugopalan, V.R. Reddy, A. Gupta, Variation of structural and hyperfine parameters in nanoparticles of Cr-substituted Co-Zn ferrites, Physical Review B, 75 (2007) 144419.
[90] Seung Wha Lee, Sung Baek Kim, Geun Young Ahn and Chul Sung Kim, J. Korean Phys. Soc, (2000) 443-446.
[91] Clare P. Marshall, W. A. Dollase, Am. Mineral., (1984) 928-936.
[119] A. Ghatage, S. Choudhari, S. Patil, S. Paranjpe, X-ray, infrared and magnetic studies of chromium substituted nickel ferrite, Journal of materials science letters, 15 (1996) 1548-1550.
[120] P. Hankare, V. Vader, N. Patil, S. Jadhav, U. Sankpal, M. Kadam, B. Chougule, N. Gajbhiye, Synthesis, characterization and studies on magnetic and electrical properties of Mg ferrite with Cr substitution, Materials Chemistry and Physics, 113 (2009) 233-238.
[121] K.M. Batoo, S. Kumar, C.G. Lee, Influence of Al doping on electrical properties of Ni–Cd nano ferrites, Current Applied Physics, 9 (2009) 826-832.
[122] A.E. Lavat, E.J. Baran, Structural and IR-spectroscopic characterization of some new Sr_2LnSbO_6 perovskites, Journal of Alloys and Compounds, 460 (2008) 152-154.
[128] E.L. Foletto, S. Battiston, J.M. Simões, M.M. Bassaco, L.S.F. Pereira, É.M. de Moraes Flores, E. Müller, Synthesis of $ZnAl_2O_4$ nanoparticles by different routes and the effect of its pore size on the photocatalytic process, Microporous and Mesoporous Materials, (2012).
[131] X. Li, Z. Zhu, Q. Zhao, L. Wang, Photocatalytic degradation of gaseous toluene over $ZnAl_2O_4$ prepared by different methods: A comparative study, Journal of hazardous materials, 186 (2011) 2089-2096.

[132] W.-C. Lin, W.-D. Yang, S.-Y. Jheng, Photocatalytic degradation of dyes in water using porous nanocrystalline titanium dioxide, Journal of the Taiwan Institute of Chemical Engineers, 43 (2012) 269-274.
[135] C.-H. Liang, M.-F. Hou, S.-G. Zhou, F.-B. Li, C.-S. Liu, T.-X. Liu, Y.-X. Gao, X.-G. Wang, J.-L. Lü, The effect of erbium on the adsorption and photodegradation of orange I in aqueous Er^{3+}-TiO_2 suspension, Journal of hazardous materials, 138 (2006) 471-478.

The scientific activity

The results obtained were valued in 5 scientific papers, of which 2 articles have been published in internationally recognized journals and the other 3 are under revision. In addition, during the 3 years of research, the results have been presented at national and international conferences.

During the three years of study I have benefited from an transnational mobility, funded by the project, within the laboratory MACS - Avancés Matériaux pour la Santé et la Catalyse, "Institut Charles Gerhardt" l'Ecole Nationale Supérieure of Chemistry, Montpellier, France.

1. List of publications

1) **Influence of chromium ion substitution on the structure and properties of zinc ferrite synthesized by the sol–gel auto-combustion method**

A.I. Borhan, T. Slatineanu, A.R. Iordan, M.N. Palamaru, *Polyhedron* (ISI: 1,813), Volume 56, 12 June 2013, Pages 82-89.

2) **Correlation between structural, magnetic and electrical properties of nanocrystalline Al^{3+} substituted zinc ferrite**

A.I. Borhan, A.R. Iordan, M.N. Palamaru, *Materials Research Bulletin* (ISI: 1,913), Volume 48, Issue 7, July 2013, Pages 2549-2556.

3) Cr^{3+} and Al^{3+} co-substituted zinc ferrite: structural analysis, magnetic and electrical properties

A.I. Borhan, A.R. Iordan, V. Hulea, M.N. Palamaru, *Polzhedron* (ISI: 1,863), (trimis spre publicare).

4) Photocatalytic activity of spinel $ZnFe_{2-x}Cr_xO_4$ nanoparticles on removal Orange I azo dye from aqueous solution,

A.I. Borhan, P. Samoila, Vasile Hulea, A.R. Iordan, M.N. Palamaru, *Journal of Taiwan Institute of Chemical Engineers* (ISI: 2,084) (sub revizie).

5) Effect of Al^{3+} substituted zinc ferrite on photocatalytic degradation of Orange I azo dye

A.I. Borhan, P. Samoila, Vasile Hulea, A.R. Iordan, M.N. Palamaru, *Journal of Photochemistry and Photobiology A: Chemistry* (ISI:2,416) (sub revizie).

2. Participation with scientific papers at national and international conferences

1. International Conference of Applied Sciences (CISA), Chemistry and Chemical Engineering, Bacău, 28-29 Aprilie 2011

Synthesis and structural characterisation of chromium-substituted zinc-ferrites (poster)

Adrian-Iulian BORHAN, Tamara Slatineanu, Alexandra Raluca Iordan, Mircea Nicolae Palamaru

2. Sesiunea jubiliara de comunicari stiintifice a studentilor, masteranzilor si doctoranzilor, Universitatea "Al. I. Cuza" Iaşi, 24 Iunie 2011

New aspects in the synthesis of chromium based spinels (poster)

Adrian-Iulian BORHAN, Tamara Slatineanu, Alexandra Raluca Iordan, Mircea Nicolae Palamaru

3. Annual Conference of doctoral schools "Alexandru Ioan Cuza" University of Iasi, Romania 21-22 October 2011

New aspects in the synthesis of chromium based spinels (prezentare orală)

A.I. Borhan, T. Slatineanu, A.R. Iordan, M.N. Palamaru

4. Sesiunea de comunicari stiintifice, Facultatea de Chimie, UAIC, Iaşi, 28 Octombrie 2011

Compuşi oxidici de tip spinel pe bază de crom (prezentare orală)

Adrian-Iulian BORHAN, Tamara Slatineanu, Alexandra Raluca Iordan, Mircea Nicolae Palamaru

5. Annual Conference of doctoral schools (Complementary modules addressed to the PhD students) "Alexandru Ioan Cuza" University of Iasi, Romania 14-16 February 2012

Effect of chromium ion substitution on electromagnetic properties of zinc ferrites (prezentare orală)

A.I.Borhan, T. Slatineanu, A.R Iordan, M. N. Palamaru

6. International Conference of Applied Sciences, Chemistry and Chemical Engineering (CISA), Bacău, 24-27 April 2012

Effect of chromium ion substitution on the electromagnetic properties of zinc ferrites (poster)

A.I.Bohan, T. Slatineanu, A.R Iordan, M. N. Palamaru

7. Sesiunea de comunicari ştiintifice, Facultatea de Chimie, Iaşi, 25Octombrie 2012

Influence of aluminium ion substitution on electromagnetic properties of zinc ferrite (prezentare orală)

A.I.Borhan, A.R Iordan, M. N. Palamaru

8. International Conference of Applied Sciences. Chemistry and Chemical Engineering (CISA), Bacău, 15-18 Mai 2013

Photocatalytic activity of $ZnFe_{2-x}Cr_xO_4$ nanoparticles on removal Orange I azo dye from aqueous solution (poster)

A.I. Borhan, P. Samoila, Vasile Hulea, A.R. Iordan, M.N. Palamaru

9. Sesiunea ştiinţifică a studenţilor, masteranzilor şi doctoranzilor, Universitatea "Alexandru Ioan Cuza" Iaşi, Romania, 28 Iunie 2013.

Activitatea fotocatalitică a nanoparticolelor din seria $ZnFe_{2-x}Cr_xO_4$ în îndepărtarea colorantului Orange I din soluţii (prezentare orală)

A.I. Borhan, P. Samoila, Vasile Hulea, A.R. Iordan, M.N. Palamaru